Numerical analysis of the beam-column connection stiffness in precast concrete with welded steel angle.

F. M. Carvalho[1], A. T. de Albuquerque[1], M. S. Medeiros Jr.[1], A. M. C. de Melo[1]

[1]*Dept. of Structural Engineering and Civil Construction*
Campus do Pici, Bloco 733 - CEP 60455-900 - Fortaleza, Ceará - Brazil
felipe.melo.7717@gmail.com, augusto.albuquerque@ufc.br, marcelomedeiros@ufc.br, macario@ufc.br

Abstract. Pre-fabricated structures present a discontinuity in the connections between the elements, such as between beam and column. This has become an important object of study, where we seek to improve the continuity of these regions, increasing the stiffness of the connection. Therefore, the objective of this study is to analyze, using numerical methods, the stiffness of the beam-column connection in precast concrete using a steel angle welded to the beams and column. To achieve this goal, a structural system composed of two beams and a column with the steel angle welded to the elements in the connection region will be modeled using the Finite Element Method. The angle is employed to assure a level of continuity in the connections between structural elements and increase its rigidity hence creating a semi-rigid condition. The result of the numerical model will be verified with a proposed analytical model, considering the existence of a spring in the connection that guarantees increased stiffness, reducing rotation in the support. Finally, the results demonstrate that the application of the welded angle on the beam and column presents better performance for semi-rigid connection, bringing greater rigidity to the connection, and reducing the existing rotation.

Keywords: Precast Concrete; Beam-column Connection; Numerical Analysis.

1 Introduction

Pre-fabricated structures offer distinct advantages over conventional structures like reinforced concrete, primarily due to the rigorous technological control of structural elements, quicker construction times, and enhanced system durability. However, this construction method requires special attention to the connections between structural elements, which bear higher stress concentrations.

The manual developed by the *Precast/Prestressed Concrete Institute* (PCI) defines that beam-column connections in precast concrete must meet several design criteria, such as strength, ductility, durability, fire resistance, and constructability [1].

A key example is the beam-column connection, typically made using concrete or metallic corbels associated with the column. These connections support the beam and were traditionally viewed as pinned connections [2]. Recent studies, however, indicate that these connections possess some degree of flexural rigidity and strength, thus exhibiting semi-rigid behavior [3].

While simplifications in calculations can be effective, they do not always equate to economic efficiency. Utilizing a semi-rigid connection can reduce labor costs for implementing a rigid connection or allow for smaller structural dimensions when using a pinned connection.

In practice, analyzing the stiffness of a precast concrete beam-column connection often involves experimental tests. However, these tests can be costly and complex due to the need for full-scale testing. As a result, the structural behavior of connections is frequently idealized using simplifications that consider them either rigid or pinned.

A more common alternative is computational analysis using Finite Element Method (FEM) software. FEM is a numerical method widely employed in engineering to solve complex problems, particularly in structural analysis.

The development of good connections between structural elements can lead to the economic and functional success of a precast concrete structure. The design of these structures involves not only appropriately sizing the dimensions but also understanding and optimizing the load path through the connection [4].

Therefore, the primary objective of this work is to conduct a numerical analysis, utilizing the Finite Element Method, to assess the stiffness of a precast concrete beam-column connection with the application of welded steel angles on the beams and columns.

2 Methodology

2.1 Computational Modeling

For the computational modeling using FEM, the Abaqus software was used. A column with a square cross-section of dimensions 50x50 cm and a height of 2.25 m, and two beams with a rectangular cross-section with a height of 25 cm, a width of 90 cm, and a length of 2.30 m were modeled. For the column, four 32 mm bars were used for the main reinforcement and 8 mm stirrups were placed along the column at 15 cm intervals. For the beam, the main reinforcement is positioned at the top layer due to negative moment loading. Five 20 mm bars were used for this, with five 8 mm bars used as stirrup supports, and 8mm stirrups placed along the beam at 15 cm intervals.

In the column, a metallic corbel with an unequal leg steel angle cross-section of dimensions 152x102 mm, thickness of 12.7 mm, and length of 80 cm was used. Additionally, two stiffeners were applied to increase the rigidity of the piece. Two equal leg steel angles were also welded to the top face of the two beams and the sides of the column, with dimensions of 72.6 mm, thickness of 12.7 mm, and length of 1 m. These angles assist in stabilizing the beams during HC erection, in addition to contributing to the resistance of negative moments [5]. Figure 1 shows the arrangement of the elements of the proposed structural system.

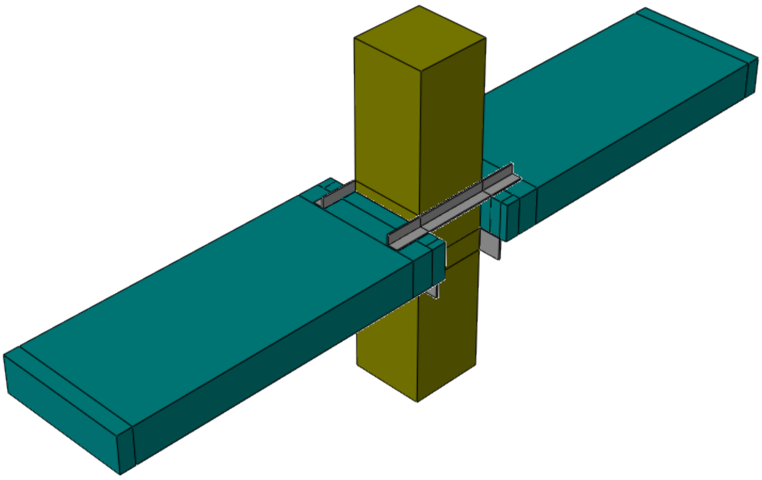

Figure 1. Configuration of the proposed structural system

In this model, only the elastic properties of the concrete were used, which are: density of 2400 kg/m³, modulus of elasticity of 31.6 GPa, and Poisson's ratio of 0.2. For the steel, the elastic and plastic properties of A36 steel were applied, which are: density of 7850 kg/m³, modulus of elasticity of 200 GPa, Poisson's ratio of 0.3, stress of 250 MPa for 0 strain, and stress of 400 MPa for 0.15 strain.

The model used presents a considerable amount of contact between the structural pieces; thus, it is necessary to determine each of the interaction conditions between these regions. The contact zones are shown in Figure 2.

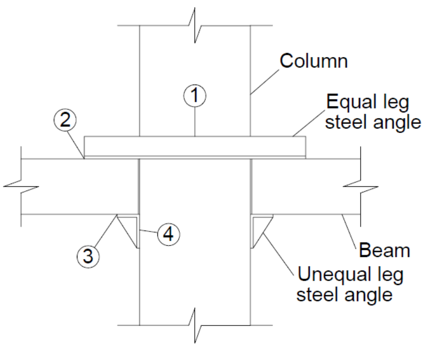

Figure 2. Contact zones of the structural model

For contacts 1 (equal leg steel angle and column), 2 (equal leg steel angle and beams), and 4 (unequal leg steel angle and column), a tie constraint was created. This constraint functions to unite the two surfaces of different regions so that they move together as if they were a single body, maintaining fixed relative positions during the analysis. This was done to ensure that the equal leg steel angle remains welded to the beams and column and that the unequal leg steel angle remains attached to the column.

For contact 3, an interaction with normal behavior of the ”Hard” contact type was created, preventing one part from penetrating the other, and with tangential behavior of the frictionless type, considering the absence of friction, since it was not measured experimentally. The same consideration was also made for the end of the beam nearly in contact with the column.

Additionally, an embedded constraint was created for the reinforcements, ensuring that they are embedded within the concrete of the beams and columns. This constraint serves to ensure that the reinforcements follow the displacements and rotations of the body in which they are embedded.

Regarding boundary conditions, a fixed support was applied to the bottom face of the column to simulate the behavior of a foundation. A displacement of 20 mm was also applied to the extreme faces of the beams.

For the finite element mesh, C3D8R elements were used for the beam, column, and equal leg steel angle. This element has 8 nodes and 3 degrees of freedom at each node, and it has reduced integration, which minimizes computational cost and the risk of locking. It is recommended for three-dimensional structural analyses, which is the case here.

For the unequal leg steel angle, C3D4 elements were used. The complex geometry of this piece did not allow for the use of the C3D8R element, necessitating the use of the C3D4 element, which is the most suitable in these cases. This element has 4 nodes with 3 degrees of freedom at each node and uses full integration. Its precision is lower than that of other elements, but since the main focus is on the analysis of the beam, the results of the analysis of the bracket do not need to be as precise.

Finally, for the reinforcements, T3D2 elements were used, which are three-dimensional truss elements with 2 nodes and 3 degrees of freedom at each node. They are very accurate for analyses of bars subjected to axial forces (tension or compression), as is the case with the reinforcements in the beams and column.

For the element size, mesh convergence tests were conducted until a size was reached where the results were close and did not generate a high computational cost. After the modeling was completed and the model was submitted, a comparison was made with the proposed theoretical model to verify the analysis results.

2.2 Analytical Analysis

The analytical model was based on the component method, as developed by Ferreira [6]. The objective of this method is to develop equations to obtain the flexural deformability due to the rotation caused by a negative moment in the connection.

The deformability of a connection is the relationship between the relative displacement of the elements that compose the connection and the applied force in the direction of that displacement [7]. We can present the following mathematical definition for the deformability and stiffness of the connection as:

$$\lambda_\phi = \frac{\phi}{M} \tag{1}$$

Here, λ_ϕ represents the deformability due to the bending moment in the beam-column connection, ϕ is the rotation in the connection, M is the bending moment applied to the connection.

The figure 3 shows the force diagram applied to the connection (a) and the rigid-body displacement experienced by the body (b). The end of the corbel is considered the center of rotation of the rigid body.

The forces F_1 and F_2 represent the effect of the welded steel angle, depicted as springs in the diagram. The force F_t is the tensile force resisted by the steel, and F_c is the compressive force resisted by the concrete. The height h_1 is the height of the beam, the length h_2 corresponds to the end of the beam supported on the column, and z is the lever arm that generates the moment M_L. We can apply moment equilibrium at the center of rotation and considering that $F_t = F_c$, and that $M_L = F_t z = F_c z$, we have:

$$F_1 h_1 + F_2 h_2 = M_L \tag{2}$$

The deformability in the connection is given by $\lambda_{\phi_L} = \phi_L / M_L$. In this equation, the value of ϕ_L can be

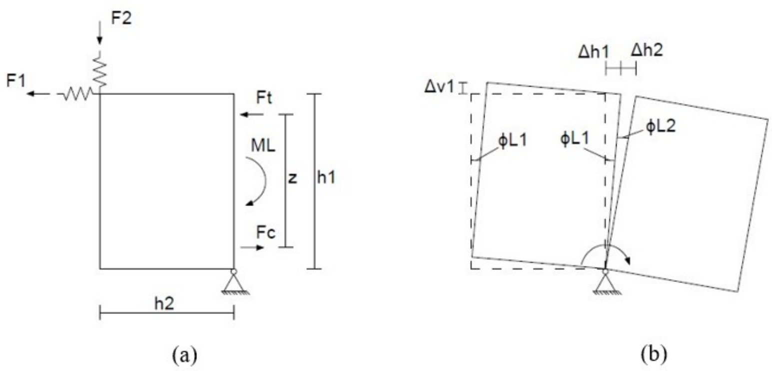

Figure 3. (a) Mechanical model; (b) Rigid body displacement.

separated into two parts, as shown in Figure 3: ϕ_{L_1}, which corresponds to the rotation in the joint region, and ϕ_{L_2}, which corresponds to the rotation due to the deformation of the beam reinforcement.

The value of Δh_1 and Δv_1 correspond, respectively, to the horizontal deformation in the angle bracket and the bending deformation. Meanwhile, Δh_2 corresponds to the horizontal deformation in the beam reinforcement. The equations to obtain these values are:

$$\Delta h_1 = \frac{L_b F_1}{E_s A_{sa}} \tag{3}$$

$$\Delta v_1 = \frac{L_b^3 F_2}{E_s A_s} \tag{4}$$

$$\Delta h_2 = \frac{L_{br} F_t}{12 E_s I_{sa}} \tag{5}$$

In this case, L_b refers to the space existing between the beam and the column, where a value of 6.35 mm was adopted, and L_{br} is specified, as provided by Ferreira [6], as the anchorage length of the reinforcement in concrete, which according to NBR 6118 [8] is given by 10ϕ.

For small displacements, which is the case here, we can state that $\Delta v_1/h_2 = \Delta h_1/h_1$. From these equations, making the necessary substitutions, we can arrive at the following deformability equations:

$$\lambda_{\phi_1} = \frac{L_b^3}{E_s(A_{sa} h_1^2 L_b^2 + 12 I_{sa} h_2^2)} \tag{6}$$

$$\lambda_{\phi_2} = \frac{L_{br}}{A_s E_s h_1 z} \tag{7}$$

The total flexural deformability in the connection is given by the sum of the values of equations 6 and 7, and the flexural stiffness in the connection is given by the inverse of this deformability.

3 Results

Firstly, based on the finite element mesh convergence study, a mesh element size of 30 mm was determined for the computational analysis. This size provides converging results and also avoids high computational costs.

The computational modeling made it possible to plot the moment-rotation curve of the analyzed model. The linear behavior extends up to the sixth point in the graph. By calculating the slope of the line connecting the first point (0,0) to the sixth point (0.001964267, 158.99693), we obtain a value of 8.09E+07, which corresponds to the computational secant stiffness of this model ($K_{SecComp}$).

From the analytical analysis, the total deformability value (λ_{ϕ_L}) found is 1.33E-8. The stiffness is given by the inverse of the deformability value, thus the analytical stiffness K_{ana} is 7.51E+07.

Figure 4 shows the behavior of the curve obtained from computational modeling and also includes the line obtained based on the slope given by the secant stiffness of the analytical model.

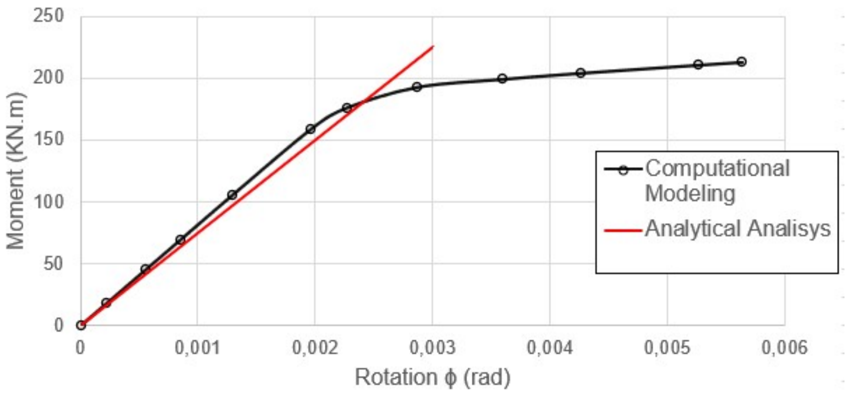

Figure 4. Computational moment-rotation curve.

Graphically, it can be observed that the two curves exhibit a very similar behavior in the linear phase. Comparing the stiffness value obtained from computational modeling with the stiffness obtained from the component method (analytical model), we have a difference of approximately 7.17%. Thus, as we obtained a low difference, the verification step of the system can be concluded, and further analyses can proceed.

Furthermore, the analysis of Von Mises stresses provides an indication of the potential failure locations in the structural element. From the FEA, we can visualize the points with the highest concentration of Von Mises stresses. The location with the highest concentration of these stresses is in the Figure 5, it shows the (a) Location of the equal leg steel angle in the structural system, (b) the Rear view of the distribution of Von Mises stresses in the equal leg steel angle and (c) Bottom view of the distribution of Von Mises stresses in the equal leg steel angle.

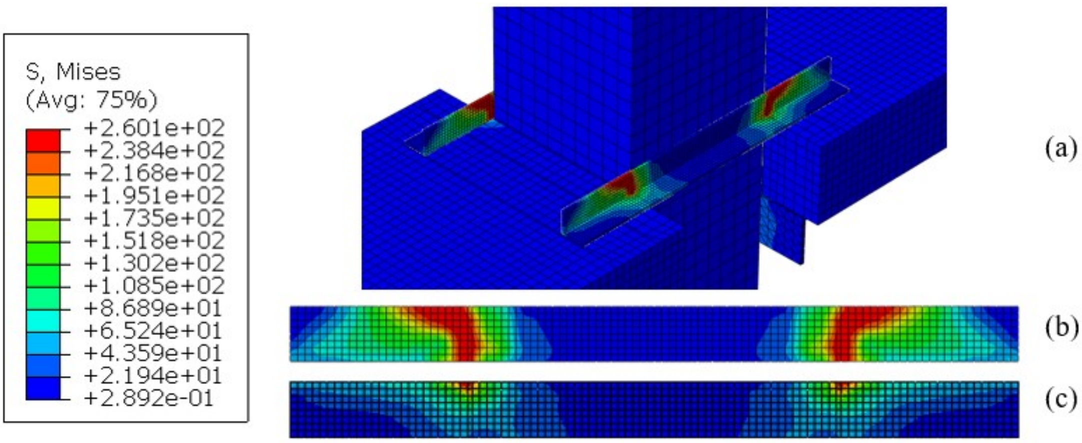

Figure 5. (a) The Location of equal leg steel angle, (b) Rear view and (c) Bottom view of Von Mises stresses.

It can be observed that the highest Von Mises stresses found in the equal-leg angle are around 260.1 MPa, which exceeds the yield stress for the adopted steel (A36 steel with $f_y = 250$ MPa). Thus, the material begins to work in the plastic phase, compromising the safety and functionality of the connection. The highest concentration of these stresses is located on the upper part of the side flange of the steel angle, just after the connection with the column. This location is precisely where a spring was assumed to exist in the mechanical model.

4 Conclusions

Therefore, the proposed computational model showed good results when compared to the analytical data obtained using the component method. Consequently, various types of data derived from computational analysis can be analyzed.

One of the key findings was the Von Mises stresses, which were prominently present in the equal-leg angle. It was observed that this component, being the most stressed by these forces, requires careful dimensioning to ensure it does not reach excessively high-stress levels.

Thus, we can conclude that the proposed connection, validated through computational analysis and comparison with an analytical model, exhibits efficient semi-rigid characteristics. Proper dimensioning of the beam-column connection mechanisms is essential moving forward.

Acknowledgements. The authors would like to acknowledge the support provided for this and other research endeavors by the Federal University of Ceará (UFC) and the funding agency Funcap (Foundation for the Support of Scientific and Technological Development of Ceará).

Authorship statement. The authors hereby confirm that they are the sole liable persons responsible for the authorship of this work and that all material that has been herein included as part of the present paper is either the property (and authorship) of the authors or has the permission of the owners to be included here.

References

[1] Precast/Prestressed Concrete Institute. *PCI Design Handbook, 7th Edition*. Precast/Prestressed Concrete Institute, 2010.

[2] F. A. Athar, Z. Ibrahim, A. A. Almohagry, M. U. Hanif, and A. Zaki. Finite element modelling of semi-rigid beam to column connection with partly hidden corbel. In *Advances in Engineering Research*, icositea-20. Atlantis Press, 2021.

[3] A. M. Miotto and M. K. E. Debs. Ligações viga-pilar de estruturas de concreto pré-moldado, análise com ênfase na deformabilidade ao momento fletor. Master's thesis, Escola de engenharia de São Carlos, Universidade de São Paulo, 2002.

[4] C. Dolan, J. Stanton, and R. Anderson. Moment resistant connections and simple connections. *PCI Journal*, vol. 32, pp. 62–74, 1987.

[5] E. Henin. Efficient precast/prestressed floor system for building. Master's thesis, The University of Nebraska - Lincoln, 2012.

[6] M. A. Ferreira and M. K. E. Debs. Estudo de deformabilidade de ligações para análise linear em pórticos planos de elementos pré-moldados de concreto. Master's thesis, Universidade de São Paulo, Sao Carlos, 1993.

[7] M. K. El Debs. *Concreto pré-moldado: fundamentos e aplicações*, 2000.

[8] Associação Brasileira de Normas Técnicas. *NBR 6118:2023 - Projeto de Estruturas de Concreto - Procedimento*. ABNT, Rio de Janeiro, Brazil, 2023.